

aggregate as bundles. Since all the strong columnar dipoles are oriented in the same direction, intense anisotropy exists that can in principle expand to macroscopic levels. Growing monocrystals of such materials is now possible. We will soon be in a position to find out if highly polarized nanotubes can be used in devices to rectify current or display unexpected properties.^[11] Our approach allows us to control precisely the internal diameter of the tube simply by modifying the positions and number of alkenes inside the monomers. We have prepared the higher C_3 symmetric lactam homologue, which incorporates conjugated dienes rather than simple conjugated alkenes; its crystal structure should yield further information about the capacity of conjugation to provide adequate rigidity to the tube units.

Received: June 11, 2001

Revised: October 15, 2001 [Z17261]

- [1] J.-M. Lehn, *Pure Appl. Chem.* **1978**, *50*, 871–892.
- [2] G. M. Whitesides, J. P. Mathias, C. T. Seto, *Science* **1991**, *254*, 1312–1319.
- [3] K. Müller-Dethlefs, P. Hobza, *Chem. Rev.* **2000**, *100*, 143–167.
- [4] B. Eisenberg, *Acc. Chem. Res.* **1998**, *31*, 117–123.
- [5] G. W. Gokel, O. Murillo, *Acc. Chem. Res.* **1996**, *29*, 425–432.
- [6] M. R. Ghadiri, J. R. Granja, L. K. Buehler, *Nature* **1994**, *369*, 301–304.
- [7] T. D. Clark, L. K. Buehler, M. R. Ghadiri, *J. Am. Chem. Soc.* **1998**, *120*, 651–656.
- [8] D. Ranganathan, V. Haridas, C. S. Sundari, D. Balasubramanian, K. P. Madhusudan, R. Roy, I. L. Karle, *J. Org. Chem.* **1999**, *64*, 9230–9240.
- [9] D. Ranganathan, C. Lakshmi, I. L. Karle, *J. Am. Chem. Soc.* **1999**, *121*, 6103–6107.
- [10] D. T. Bong, T. D. Clark, J. R. Granja, M. R. Ghadiri, *Angew. Chem.* **2001**, *113*, 1016–1041; *Angew. Chem. Int. Ed.* **2001**, *40*, 988–1011.
- [11] P. K. Kienker, W. F. DeGrado, J. D. Lear, *Proc. Natl. Acad. Sci. USA* **1994**, *91*, 4859–4863.
- [12] T. D. Clark, J. M. Buriak, K. Kobayashi, M. P. Isler, D. E. McRee, M. R. Ghadiri, *J. Am. Chem. Soc.* **1998**, *120*, 8949–8962.
- [13] L. Tomasic, G. P. Lorenzi, *Helv. Chim. Acta* **1987**, *70*, 1012–1016.
- [14] D. Seebach, J. L. Matthews, A. Meden, T. Wessels, C. Baerlocher, L. B. McCusker, *Helv. Chim. Acta* **1997**, *80*, 173–182.
- [15] J. L. Matthews, K. Gademann, B. Jaun, D. Seebach, *J. Chem. Soc. Perkin Trans. 1* **1998**, 3331–3340.
- [16] M. R. Ghadiri, J. R. Granja, R. A. Milligan, D. E. McRee, N. Khazanovich, *Nature* **1993**, *366*, 324–327.
- [17] J. D. Hartgerink, J. R. Granja, R. A. Milligan, M. R. Ghadiri, *J. Am. Chem. Soc.* **1996**, *118*, 43–50.
- [18] V. Pavone, E. Benedetti, B. DiBlasio, A. Lombardi, C. Pedone, L. Tomasic, G. P. Lorenzi, *Biopolymers* **1989**, *28*, 215–223.
- [19] J. Lowbridge, E. Mtetwa, R. J. Ridge, C. N. C. Drey, *J. Chem. Soc. Perkin Trans. 1* **1986**, 155–156.
- [20] D. N. J. White, C. Morrow, P. J. Cox, C. N. C. Drey, J. Lowbridge, *J. Chem. Soc. Perkin Trans. 2* **1982**, 239–243.
- [21] I. L. Karle, J. Karle, *Acta Crystallogr.* **1963**, *16*, 969–975.
- [22] M. Dobler, J. D. Dunitz, J. Krajewski, *J. Mol. Biol.* **1969**, *42*, 603–606.
- [23] L. Zhang, J. P. Tam, *Tetrahedron Lett.* **1997**, *38*, 4375–4378.
- [24] R. D. Allan, H. W. Dickenson, G. A. R. Johnston, R. Kazlauskas, H. W. Tran, *Aust. J. Chem.* **1985**, *38*, 1651–1656.
- [25] Crystal data for **1** (colorless): dimensions $0.15 \times 0.15 \times 0.30$ mm, triclinic, P_1 , $a = 4.726(2)$, $b = 7.709$, $c = 11.054(2)$ Å, $\alpha = 72.97(1)$, $\beta = 77.78(1)$, $\gamma = 88.55(1)^\circ$, $V = 306.1$ Å³, $Z = 1$; $\rho_{\text{calc}} = 1.286$ g cm⁻³; $2\theta_{\text{max}} = 140^\circ$; 1353 reflections (1353 independent, 1193 with $F > 2.0\sigma F$, 1353 used in refinement); 198 parameters were refined; the max. and min. electron density map were 0.241 and -0.207 e Å⁻³; the final residues were $R(F) = 0.0509$, and $R_w(F^2) = 0.1382$, GoF = 1.042.

- [26] The data were collected on a Nonius CAD4 diffractometer; $\text{Cu}_{K\alpha}$; $\lambda = 1.54184$ Å; $\omega 2\theta$ scan; 293(2) K; the structure was solved by the application of direct methods and refined using SHELX97 (G. M. Sheldrick, *Acta Crystallogr. Sect. A* **1990**, *46*, 467–473); the refinements were against $|F^2|$, the data were reduced using XCAD4 (K. Harms, S. Wocadlo, University of Marburg), all programs included in the WinGX package (L. J. Farrugia, *J. Appl. Crystallogr.* **1999**, *32*, 837–838); the H atoms were geometrically placed.
- [27] Crystallographic data (excluding structure factors) for the structures reported in this paper have been deposited with the Cambridge Crystallographic Data Centre as supplementary publication no. CCDC-164579 (**1**), -164580 (**4**), and -164581 (**5**). Copies of the data can be obtained free of charge on application to CCDC, 12 Union Road, Cambridge CB21EZ, UK (fax: (+44) 1223-336-033; e-mail: deposit@ccdc.cam.ac.uk).
- [28] Y. A. Ovchinnikov, V. T. Ivanov, *Tetrahedron* **1974**, *30*, 1871–1890.
- [29] Crystal data for **4** (colorless): Dimensions $0.05 \times 0.05 \times 0.48$ mm, monoclinic, $P2_1/a$, $a = 9.434(14)$, $b = 10.338(4)$, $c = 11.393(7)$ Å, $\beta = 111.22(6)^\circ$, $V = 1035.8$ Å³, $Z = 2$; $\rho_{\text{calc}} = 1.246$ g cm⁻³; $2\theta_{\text{max}} = 130^\circ$; 1810 reflections (1725 independent, 967 with $F > 2.0\sigma F$, 1725 used in refinement); 167 parameters were refined; the max. and min. electron density map were 0.366 and -0.217 e Å⁻³; the final residues were $R(F) = 0.0814$, and $R_w(F^2) = 0.2358$, GoF = 0.931.
- [30] Crystal data for **5** (colorless): dimensions $0.08 \times 0.17 \times 0.45$ mm, trigonal, $R3$, $a = 17.299(5)$, $b = 17.299(5)$, $c = 4.819(5)$ Å, $V = 1248.9$ Å³, $Z = 3$; $\rho_{\text{calc}} = 1.162$ g cm⁻³; $2\theta_{\text{max}} = 130^\circ$; 988 reflections (878 independent, 518 with $F > 2.0\sigma F$, 878 used in refinement); 65 parameters were refined; the max. and min. electron density map were 0.237 and -0.202 e Å⁻³; the final residues were $R(F) = 0.0937$, and $R_w(F^2) = 0.2556$, GoF = 0.991.

Single-Step, Highly Active, and Highly Selective Nanoparticle Catalysts for the Hydrogenation of Key Organic Compounds**

Robert Raja, Tetyana Khimyak, John Meurig Thomas,*
Sophie Hermans, and Brian F. G. Johnson*

More than three quarters of the organic molecular products that are manufactured industrially entail the processes of either hydrogenation or oxidation; and with the impending arrival of the so-called hydrogen economy and the parallel drive towards clean technology this fraction will inevitably rise in the near future, the most desirable agents of conversion

[*] Prof. Sir J. M. Thomas, Dr. R. Raja
The Royal Institution of Great Britain
Davy Faraday Research Laboratory
21 Albemarle Street, London W1S 4BS (UK)
Fax: (+44) 1223-339200
E-mail: has22@cam.ac.uk

Prof. Sir J. M. Thomas
Department of Materials Science and Metallurgy
New Museums Site
Pembroke Street, Cambridge CB2 3QZ (UK)

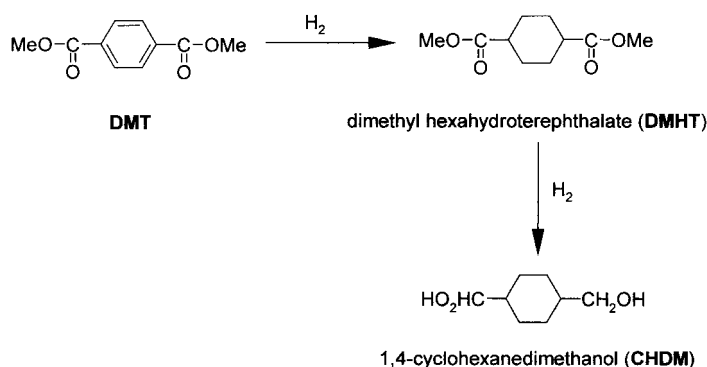
Prof. B. F. G. Johnson, Dr. R. Raja, T. Khimyak, Dr. S. Hermans
Department of Chemistry, University of Cambridge, Lensfield Road,
Cambridge CB2 1EW (UK)
Fax: (+44) 1223-339200

[**] We gratefully acknowledge the support (by a rolling grant to J.M.T. and an award to B.F.G.J.) of EPSRC (UK), of the Cambridge Overseas Trust (Schlumberger research), and ICI (for T.K.), and the award of a research fellowship (for S.H.) from Newnham College, Cambridge.

being molecular hydrogen and air (or oxygen). But increasing use of these agents requires the further development of robust, new, highly active and selective catalysts that, ideally, should effect single-step conversions under relatively mild and solvent-free conditions.^[1] Here we describe the promising performance of two, related new bimetallic nanocatalysts for the hydrogenation of:

- 1) benzoic acid to cyclohexane carboxylic acid (**1**);
- 2) dimethyl terephthalate (DMT) to 1,4-cyclohexanedimethanol (CHDM) (**2**);
- 3) naphthalene in a highly selective manner to *cis*-decalin (**3**).

It is relevant to note that **1**, upon treatment with NOHSO_4 in the presence of strong acid (such as oleum) yields caprolactam,^[2] the precursor of nylon; that **2** is preferred over ethylene glycol^[3] as a stepping stone in the production of polyester fibers for extensive use in photography, antifogging agents, and in other applications involving polycarbonates and polyurethanes;^[4] and that **3** is a useful source (and storage medium) for hydrogen. The hydrogenation of only the benzene ring in benzoic acid has scarcely been described.^[5] Likewise, the hydrogenation of DMT to dimethyl hexahydroterephthalate (DMHT, Scheme 1) has been achieved to date only with a rhodium complex tethered on silica-supported palladium.^[6]



Scheme 1. Hydrogenation of dimethyl terephthalate (DMT).

The bimetallic nanoparticle catalysts reported here are discrete anchored clusters, Ru_5Pt and $\text{Ru}_{10}\text{Pt}_2$, prepared by the gentle decarbonylation of the parent, mixed-metal precursor anions, $[\text{Ru}_5\text{PtC}(\text{CO})_{15}]^{2-}$ and $[\text{Ru}_{10}\text{Pt}_2\text{C}_2(\text{CO})_{28}]^{2-}$ (Figure 1), after first inserting them, along with their counterions into mesoporous silica, in a manner closely akin to the preparation of anchored Ru_6Sn ,^[7] Pd_6Ru_6 ,^[8] and of $\text{Cu}_4\text{Ru}_{12}$,^[9] nanoclusters described previously. The diameter of the resulting, well-dispersed, isolated and anchored bimetallic nanoparticles is in the range of approximately 10–20 Å^[10, 11] (see below).

A bright-field (BF) scanning transmission electron micrograph (Figure 2A) directly reveals the mesoporosity of the silica (MCM-41) used as host to encapsulate the bimetallic nanoparticle catalysts.^[12, 13] And a bright field/high-angle-annular dark field (BF/HAADF) pair (Figure 2B and C) shows clearly the uniform size and distribution of the denuded mixed-metal anion (in this case $\text{Ru}_{10}\text{Pt}_2$) within the mesopores. These anchored nanoparticle catalysts are readily

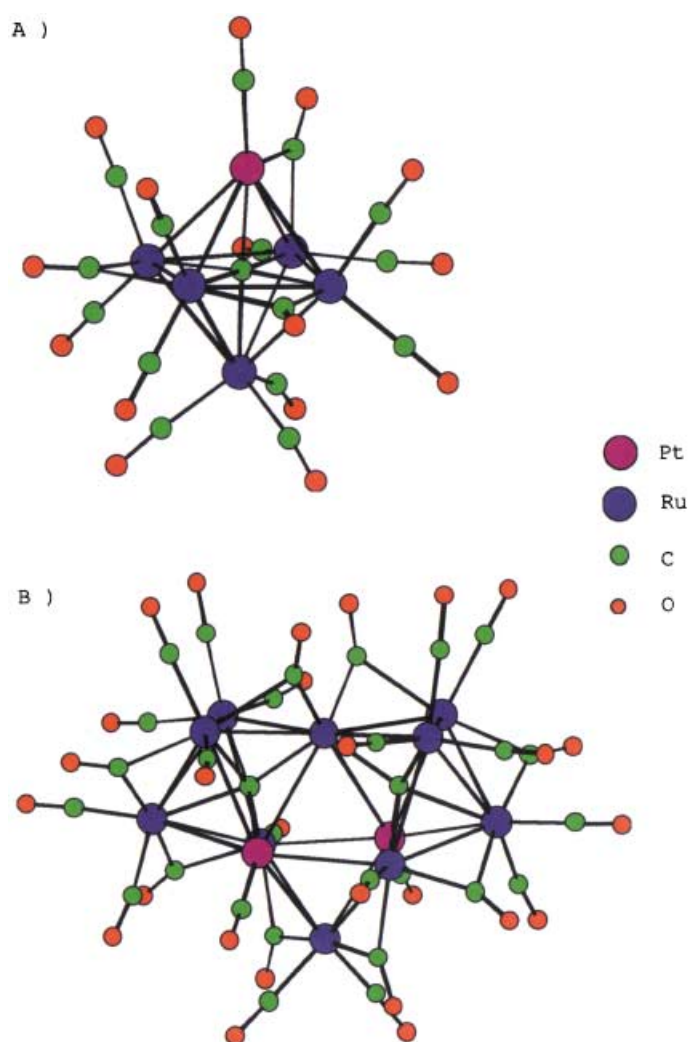


Figure 1. A) Structure of the anion in $[\text{Ph}_4\text{P}]_2[\text{Ru}_5\text{PtC}(\text{CO})_{15}]$ (**4**).^[18] B) Structure of the anion in $[\text{PPN}]_2[\text{Ru}_{10}\text{Pt}_2\text{C}_2(\text{CO})_{28}]$ (**5**; $\text{PPN} = [(\text{C}_6\text{H}_5)_3\text{P}=\text{N}=\text{P}(\text{C}_6\text{H}_5)_3]^+$), prepared and fully described as reported elsewhere.^[19]

accessible to all the reactant and product molecules of this investigation.

A preliminary test of the performance of these catalysts was carried out using cyclohexene as the reactant. The results (Table 1) leave little doubt that the catalytic activity and selectivity of both Ru_5Pt and $\text{Ru}_{10}\text{Pt}_2$ are exceptional. In the hydrogenation of naphthalene again the performance of these two catalysts is exceptional (Table 1): only the fully hydrogenated naphthalenes (decalins) are formed, and the ratio of the *cis* to the *trans* forms is high (ca. 5.5:1 to 8.6:1 depending upon the precise conditions). Moreover, these catalysts are unimpaired in their performance even when substantial amounts of a well-known “sulfur poison” is deliberately introduced—in sharp contrast to the behavior of otherwise good bimetallic nano-catalysts (Pd_6Ru_6 , Ru_6Sn , and $\text{Cu}_4\text{Ru}_{12}$) previously tested by us.

In the hydrogenation of benzoic acid the efficacy of the two RuPt nanocatalysts again surpasses that of the three, quite distinct bimetallic catalysts that we have previously described (Figure 3).

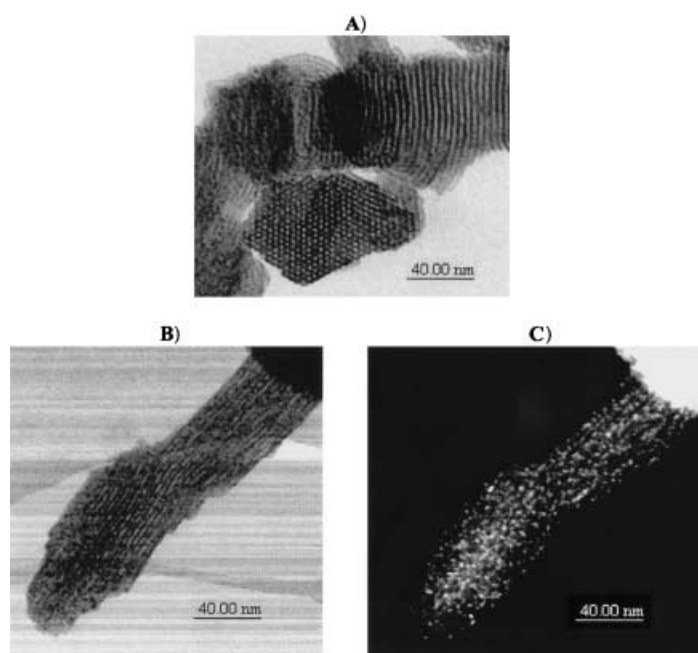


Figure 2. A) BF scanning transmission electron micrograph^[7, 12] of a typical group of crystallites of mesoporous silica (ca. 30 Å diameter) onto the inner walls of which nanoparticle arrays have been anchored (not clearly visible, see Figures 2B and C of Ru₁₀Pt₂ catalysts. B) and C) A BF/HAADF pair of another region of the mesopore-encapsulated Ru₁₀Pt₂ nanocatalysts. Whereas in (B) many of the nanoparticles are just about visible, in (C) they all stand out very clearly and are seen to be aligned along the mesopores (compare Figure 4 of ref. [7]).

The hydrogenation of DMT (see Scheme 1) to the valuable product CHDM (**2**) is carried out industrially in two steps using two reactors.^[14] The first, which requires a temperature in the range 160–180 °C and a pressure of 30–48 MPa, uses a supported Pd catalyst. This highly exothermic process yields the intermediate, dimethyl hexahydroterephthalate (DMHT).

This, in turn, is converted at about 200 °C and 40 bar (40×10^5 Pa) H₂ over a copper chromite catalyst, into the required CHDM.^[14] With our catalysts, one-step conversions of DMHT into CHDM are effected in high yield even after a mere 4 h contact time at 100 °C, a pressure of 20 bar (20×10^5 Pa) H₂, in ethanol as a benign solvent (Table 2). It is noteworthy that the yield of CHDM passes through a maximum, there being cross-linked products such as 4-methyloxymethylhydroxymethylcyclohexane and bis (4-hydroxymethylcyclohexyl) ether formed during the conversion. Other bimetallic nano-catalysts that are less efficient than Ru₅Pt or Ru₁₀Pt₂ as straightforward hydrogenation catalysts (see Table 1), species such as Cu₄Ru₁₂, are especially effective in producing good yields of CHDM (see Table 2). Kinetic studies (Figure 4 and Figure 5) reveal the changes more explicitly. It is also noteworthy that the *cis:trans* ratio of the CHDM formed is 80:20 for the Cu₄Ru₁₂ catalyst, and 65:35 in the case of both the RuPt catalysts. It augurs well here that, in the case of the Cu₄Ru₁₂ catalyst, these values are extremely significant for industrial processing (ideally 88:12).^[15, 16] Notably, the Pd₆Ru₆ catalyst produces a 50:50 mixture (*cis:trans*) of CHDM.

Given the sensitive time dependence of product yields in the (one-step) hydrogenation of DMT there is abundant scope here for the chemical engineer to optimize the production of CHDM. Further work on the structure and catalytic properties of the two compositionally identical, but elementally different, bimetallic nanoparticles, is in progress.

Experimental Section

[Ph₄P]₂[Ru₅PtC(CO)₁₅] (**4**): An excess of KOH (500 mg) was added to a solution of [Ru₅PtC(CO)₁₆] (200 mg, 0.17 mmol) in methanol. The mixture was stirred at room temperature for 2 h after which an excess of Ph₄PCl (160 mg, 0.43 mmol) was added to yield **4** as dark red precipitate. The solid was collected by filtration and washed with hexane, yield: 268 mg (87 %).

Table 1. Hydrogenation of cyclohexene and naphthalene—comparison of catalysts.

Catalyst ^[a]	Substrate	t [h]	p H ₂ [bar] ^[b]	T [K]	Conv [mol %]	TOF [h ⁻¹] ^[d]	Product distribution [mol %] ^[e]			
							A	B	C	D
Ru ₃ Pt/SiO ₂	cyclohexene	1.5	10	353	52.5	6860	100	–	–	–
		3	1		96.9	6341	100	–	–	–
Ru ₁₀ Pt ₂ /SiO ₂	cyclohexene	1.5	8	353	75.2	14530	100	–	–	–
		2	0		98.0	14201	100	–	–	–
Pd ₆ Ru ₆ /SiO ₂	cyclohexene	1.5	15	353	31.3	3250	100	–	–	–
		3	10		55.0	3015	100	–	–	–
Ru ₆ Sn/SiO ₂	cyclohexene	1.5	17	353	15.2	1989	92	–	–	11.5
		3	15		26.5	1734	85	–	–	14.7
Cu ₄ Ru ₁₂ /SiO ₂	cyclohexene	1.5	17	353	11.5	2015	89	–	–	11
		3	15		21.7	1950	80	–	–	20.2
Ru ₃ Pt/SiO ₂	naphthalene	8	8	373	31.5	792	–	84	15	–
		8 ^[c]	7		32.0	805	–	86.4	13.3	–
Ru ₁₀ Pt ₂ /SiO ₂	naphthalene	8	6	373	44.7	1660	–	89.4	10.2	–
		8 ^[c]	6		45.0	1671	–	88.5	11.3	–
Pd ₆ Ru ₆ /SiO ₂	naphthalene	8	14	373	7.0	19	–	50	34	15
		8 ^[c]	19		–	–	–	no reaction	–	–
Ru ₆ Sn/SiO ₂	naphthalene	8	12	373	9.5	238	–	48.2	45	6.5
		8 ^[c]	18		–	–	–	no reaction	–	–
Cu ₄ Ru ₁₂ /SiO ₂	naphthalene	8	19	373	–	–	–	no reaction	–	–
		8 ^[c]	18		–	–	–	no reaction	–	–

[a] The mesoporous SiO₂ used here is of the MCM-41 type. Reaction conditions: cyclohexene \approx 50 g; naphthalene \approx 8 g (dissolved in 55 g of hexadecane); catalyst = 50 mg; H₂ pressure = 20 bar. [b] Residual H₂ pressure in the reactor. [c] 200 ppm of sulfur was introduced (benzothiophene). [d] TOF = [(mol_{substr})/(mol_{cluster})⁻¹ h⁻¹]. [e] A = cyclohexane; B = *cis*-decalin; C = *trans*-decalin; D = others.

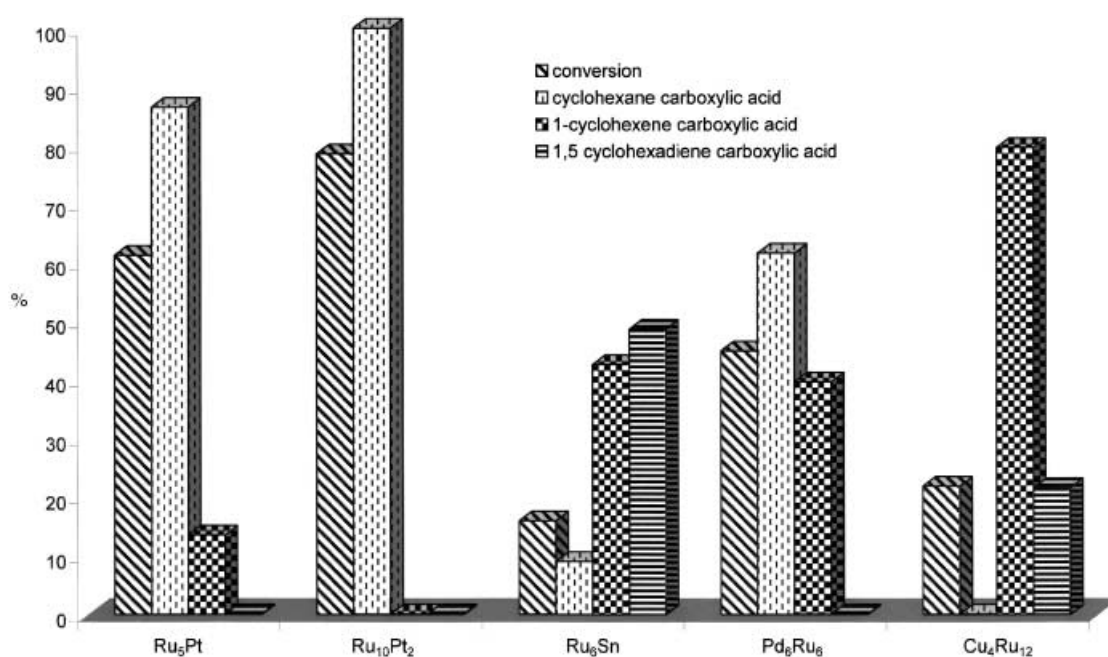


Figure 3. Bar chart of the relative performances and selectivity of the Ru_5Pt and $\text{Ru}_{10}\text{Pt}_2$ catalysts compared to other bimetallic nanocatalysts, (used by us in our previous studies^[7–9]) for the hydrogenation of benzoic acid. Note that the Ru_5Pt and $\text{Ru}_{10}\text{Pt}_2$ catalysts display a high degree of selectivity for the cyclohexane carboxylic acid in marked contrast to the other bimetallic analogues. Reaction conditions: benzoic acid ≈ 2.5 g (dissolved in 75 mL of ethanol); catalyst = 50 mg, H_2 pressure = 20 bar, $T = 373$ K; $t = 24$ h.

Table 2. Hydrogenation of dimethyl terephthalate (DMT)—comparison of catalysts.

Catalyst ^[a]	t [h]	Conv [mol %]	TOF [h^{-1}] ^[b]	Product distribution [mol %] ^[c]			
				A	B	C	D
$\text{Ru}_5\text{Pt}/\text{SiO}_2$	4	7.5	155	58.7	33.5	—	6.9
	8	18.4	191	55.3	5.2	—	39.4
	24	36.9	138	61.2	—	—	38.7
$\text{Ru}_{10}\text{Pt}_2/\text{SiO}_2$	4	23.3	714	42.6	52.3	—	—
	8	39.5	605	53.6	9.0	—	37.1
	24	67.2	443	51.4	—	—	48.5
$\text{Pd}_6\text{Ru}_6/\text{SiO}_2$	4	6.2	98	32.9	16.8	—	51.1
	8	15.5	125	22.5	4.2	—	74.2
	24	23.7	64	18.2	—	—	81.5
$\text{Ru}_6\text{Sn}/\text{SiO}_2$	4	—	—	—	—	—	—
	8	5.3	54	77.2	—	22.6	—
	24	8.0	27	81.0	—	18.6	—
$\text{Cu}_4\text{Ru}_{12}/\text{SiO}_2$	4	—	—	—	—	—	—
	8	10.4	102	22.2	54.5	23.0	—
	24	14.2	45	25.3	63.2	—	11.3

[a] The mesoporous SiO_2 used here is of the MCM-41 type. Reaction conditions: DMT ≈ 2.5 g (dissolved in 75 mL ethanol); $T = 373$ K; H_2 pressure = 20 bar; catalyst ≈ 50 mg. [b] $\text{TOF} = [(\text{mol}_{\text{substr}})(\text{mol}_{\text{cluster}})^{-1} \text{h}^{-1}]$. [c] A = dimethyl hexahydroterephthalate (DMHT); B = 1,4-cyclohexanedimethanol (CHDM); C = mixture of 4-methyl-4-cyclohexane carboxylic acid methyl ester and 1-hydroxymethyl-4-methylcyclohexane; D = mixture of 4-methoxymethylhydroxymethylcyclohexane and bis(4-hydroxymethylcyclohexyl) ether.

Elemental analysis calcd (%) for $\text{C}_{64}\text{H}_{40}\text{O}_{15}\text{P}_2\text{PtRu}_5$: C 42.44, H 2.23, P 3.42; found: C 40.62, H 2.27, P 3.42; IR (CH_2Cl_2): $\tilde{\nu}_{\text{max}} = (\text{CO})$ 1975s (br), 1911w (sh), 1823w (br), 1771w (br) cm^{-1} ; ^1H NMR (400 MHz, 300 K, CD_2Cl_2): $\delta = 7.92$ – 7.60 (m, 20H, $\text{P}(\text{C}_6\text{H}_5)_4$); ^{13}C NMR (400 MHz, 300 K, CD_2Cl_2): $\delta = 201.0$ (m, CO), 136.0–117.37 (m, C_6H_5); MS: m/z (%): 566 (100) [$M^{2-}/2$], 552 (48) [$M^{2-}/2 - \text{CO}$].

The catalytic materials were prepared by standard procedures.^[7,9] The mesoporous silica was loaded with cluster **4** or **5** by making a slurry in diethyl ether/dichloromethane. The mesopore-encapsulated clusters **4** and **5** were activated by heating at 195°C in vacuo for 2 h. As in earlier preparations,^[7] the FT-IR spectra recorded after activation showed no residual peaks corresponding to the carbonyl stretching frequencies.

The electron microscopy characterizations were carried out on a VG HB501 field-emission STEM microscope, and the catalysts dispersed

on a holey carbon film supported on a copper grid from a suspension in hexane, as described in ref. [7].

The catalytic reactions were carried out in a high-pressure stainless steel catalytic reactor lined with poly ether ether ketone (PEEK). Dry hydrogen (20 bar (20×10^5 Pa)) was pressurized into the reaction vessel and, using a mini robot liquid-sampling valve, small aliquots of the sample were removed to study the kinetics of the reaction, without perturbing the pressure in the reactor.^[17] The products were analyzed (using a suitable internal standard)^[7] by gas chromatography (GC, Varian, Model 3400 CX) employing a HP-1 capillary column (25 m \times 0.32 mm) and flame ionization detector. The identity of the products was confirmed by injecting authenticated samples and further by liquid chromatography mass spectrometry (LC-MS; Shimadzu, QP 8000) employing a gamma-cyclodextrin dialkyl column (ChiralDEX, 20 m \times 0.25 mm).

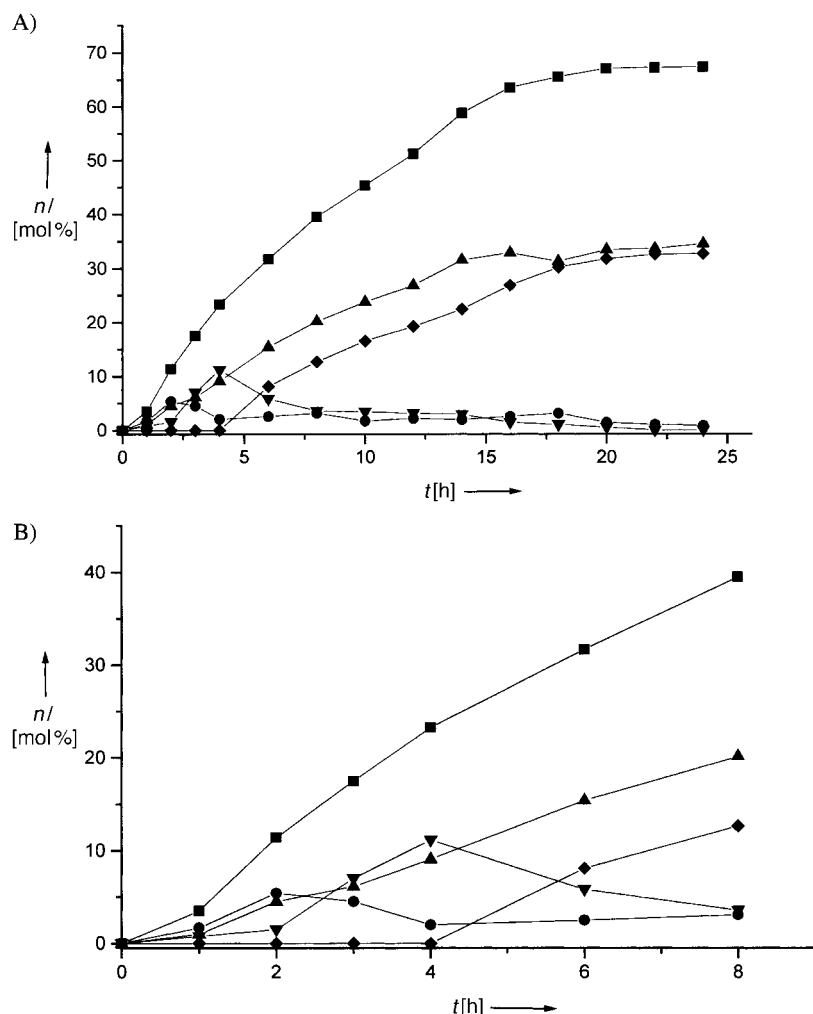


Figure 4. Kinetics of hydrogenation of DMT by using $\text{Ru}_{10}\text{Pt}_2$ (A). An expanded view of the initial part of the reaction where the formation of CHDM, after 4 h, is clearly detected is shown in (B). The CHDM further reacts in the presence of this catalyst to form coupling by-products as elaborated in Table 2 and in the text. ■ conversion of DMT; ● C (see Table 2 for details); ▲ DMHT; ▼ CHDM; ◆ D (see Table 2 for details).

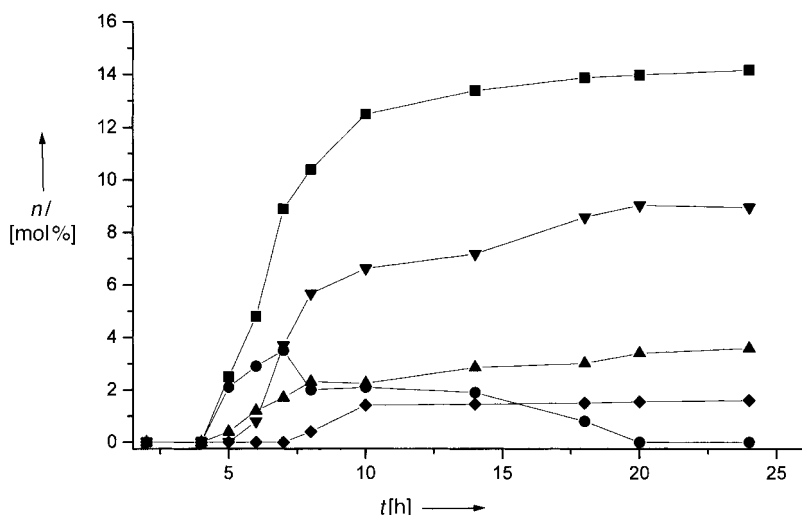


Figure 5. Kinetics of hydrogenation of DMT using $\text{Cu}_4\text{Ru}_{12}$ as the catalyst. Note that the product distribution is markedly different (c.f. Figure 4) and the formation of by-products is relatively suppressed. The synergistic role of the copper in driving the reaction further (conversion of DMHT into CHDM) is clearly evident here, in stark contrast with what is observed in Figure 4 using the $\text{Ru}_{10}\text{Pt}_2$ catalyst; ■ conversion of DMT; ● C (see Table 2 for details); ▲ DMHT; ▼ CHDM; ◆ D (see Table 2 for details).

The Ru–Pt catalysts have been re-used three times without appreciable loss in catalytic activity or selectivity. Further, experiments, analogous those reported earlier,^[7] were carried out to rule out the possibility of leaching, and analysis of the resulting filtrate at the end of reaction (24 h, for DMT hydrogenation) by ICP (ICP = inductively charged plasma) and atomic absorption spectroscopy (AAS) revealed only trace amounts (<5 ppb) of dissolved metal ions (Pt, Ru).

Received: August 13, 2001 [Z17719]

- [1] J. M. Thomas, R. Raja, G. Sankar, B. F. G. Johnson, D. W. Lewis, *Chem. Eur. J.* **2001**, 7, 2973.
- [2] J. Ritz, H. Fuchs, H. Kieczka, W. C. Morgan, *Ullmanns Encyclopedia of Industrial Chemistry*, Wiley-VCH, Weinheim, Germany, **2001**.
- [3] a) T. Mizumoto, H. Kamatani (Toyobo), JP 75142537, **1975** [*Chem. Abstr.* **1976**, 84, 135183s]; b) B. J. Sublett, G. W. Connell (Eastman Chemical), US-A 5559159, **1995** [*Chem. Abstr.* **1996**, 125, 277914v].
- [4] a) T. K. Debroy, M. Guagliardo, J. P. Pucknat (BASF), EP 262069, **1986** [*Chem. Abstr.* **1988**, 109, 56675k]; b) R. R. Amborse, J. B. O'Dwyer, B. K. Johnston, D. P. Zielinski, S. Porter, W. H. Tyger (PPG Industries) US-A 4859743, **1988** [*Chem. Abstr.* **1990**, 112, 38296v].
- [5] C. S. Chin, B. Lee, J. Moon, J. H. Song, Y. S. Park, *Bull. Korean Chem. Soc.* **1995**, 16, 528.
- [6] H. Yang, H. R. Gao, R. J. Angelici, *Organometallics* **2000**, 19, 622.
- [7] S. Hermans, R. Raja, J. M. Thomas, B. F. G. Johnson, G. Sankar, D. Gleeson, *Angew. Chem.* **2001**, 113, 1251–1255; *Angew. Chem. Int. Ed.* **2001**, 40, 1211–1215.
- [8] R. Raja, S. Hermans, D. S. Shephard, S. Bromley, J. M. Thomas, B. F. G. Johnson, T. Maschmeyer, *Chem. Commun.* **1999**, 2131.
- [9] D. S. Shephard, T. Maschmeyer, G. Sankar, J. M. Thomas, D. Ozkaya, B. F. G. Johnson, R. Raja, R. D. Oldroyd, R. G. Bell, *Chem. Eur. J.* **1998**, 4, 1214.
- [10] J. M. Thomas, *Angew. Chem.* **1999**, 111, 3800; *Angew. Chem. Int. Ed.* **1999**, 38, 3588.
- [11] W. Zhou, J. M. Thomas, D. S. Shephard, B. F. G. Johnson, D. Ozkaya, T. Maschmeyer, R. G. Bell, Q. Ge, *Science* **1998**, 280, 705.
- [12] D. Ozkaya, W. Zhou, J. M. Thomas, P. A. Midgeley, V. J. Keast, S. Hermans, *Catal. Lett.* **1999**, 60, 113.
- [13] J. M. Thomas, O. Terasaki, P. L. Gai, W. Zhou, J. Gonzalez-Calle, *Acc. Chem. Res.* **2001**, 34, 583.
- [14] a) M. L. Schlossman (Tevco), US-A 4301046, **1981** [*Chem. Abstr.* **1982**, 96, 24664c]; b) P. Appleton, M. A. Wood (Eastman Chemical), US 5414159, **1993** [*Chem. Abstr.* **1995**, 123, 170535d].
- [15] P. Werle, M. Morawietz, *Ullmanns Encyclopedia of Industrial Chemistry*, Wiley-VCH, Weinheim, Germany, **2001**.
- [16] R. D. Adams, W. Wu, *J. Cluster Sci.* **1991**, 2, 271–290.
- [17] J. M. Thomas, R. Raja, G. Sankar, R. G. Bell, *Acc. Chem. Res.* **2001**, 34, 191.
- [18] The single-crystal X-ray structure of **4** will be reported elsewhere.
- [19] B. F. G. Johnson, S. Hermans, T. Khimyak, *Organometallics* **2001**, submitted.